

DISTRIBUTION OF IMPACT MELT GENERATED BY THE SOUTH POLE-AITKEN IMPACT

K. Uemoto¹, M. Ohtake², Y. Yokota³, S. Yamamoto³, R. Nakamura⁴, J. Haruyama², T. Matsunaga³, Y. Ishihara², T. Iwata². ¹Tokyo Univ. (uemoto@planeta.sci.isas.jaxa.jp), ²Japan Aerospace Exploration Agency(JAXA), ³National Institute for Environmental Studies, ⁴National Institute of Advanced Industrial Science and Technology.

Introduction: The South Pole-Aitken (SPA) basin is one of the largest basins on the Moon. It was determined to have an elliptical structure with a 2400 km major axis and a 2050 km minor axis in a recent study [1]. The basin impact is very large, so it has been suggested that most of the crustal material within the SPA was excavated [2], or in other words, it is possible that the mantle materials have been exposed within the basin. However, the mantle materials may not be exposed everywhere inside the basin. Therefore we investigated the central area of the basin because the basin excavation was the deepest in the central area and offers a high probability that the mantle materials are exposed. However, because the basin impact is very large, the materials in the central area should have melted [e.g., 3]. A previous study using a numerical simulation of the formation of the SPA indicated that the impact melt generated by the SPA basin impact and mantle material melted to about a 700 km depth [4]. A previous study determined that the final depth of the impact melt after basin transition was about 50 km [5]. Therefore, exposed mantle materials in the central area of the basin would have melted. Mineralogical and geological understanding of the SPA interior is limited because it is one of the oldest basins (pre-Nectarian in age [6]), and its surface has become obscured by intensive cratering and mixing since its formation. Therefore, it is hard to identify areas where the impact melt has been exposed. However, we used a new mineralogical map based on high-spatial-resolution reflectance spectra using the SELENE (Kaguya) Multiband Imager (MI) [7]. In our previous research, we identified a central depression where the impact melt of the SPA had pooled (162.6°E, 53.7°S, 315 and 343 km radius) [8]. However, in [8], we still had not identified the location of exposed impact melt on the basin surface. Now, we use new spectral data from MI to investigate the distribution of the impact melt.

Methods: It is suggested that high-Ca pyroxene (HCP) dominant area expand in the central area of SPA, and it is possible that this area is impact melt [8]. However, previous studies have suggested that a 'cryptomare' expanded within the center of the SPA basin [9], and the pyroxenes of mare basalt have high-Ca composition [10]. Thus, we should identify the distribution of HCP layer. And we distinguished between mare and impact melt by estimating the area, thickness and chemical abundance of the respective layers.

Seven thousand Kaguya MI map data files [7] with a spatial resolution of 14 m/pixel are used to generate a binned low-resolution MI reflectance map (237 m/pixel) within the center of the SPA basin (around the central depression from [8], at 40 to 70°S and 140 to 220°W). The wavelength assignment of MI provides both visible and near-infrared coverage in spectral bands of 415, 750, 900, 950, 1000, 1050, 1250, and 1550 nm. Mineral phases have diagnostic absorption features, depending on the minerals. We made a color composite image from these data (RGB map). The colors were assigned to continuum-removed absorption depths to generate these images: red for 900 nm (Low-Ca pyroxene (LCP)), green for 1050 nm (olivine or HCP), and blue for 1250 nm (plagioclase). In addition, we made iron (FeO) and titanium (TiO₂) abundance maps using the Lucey method [11] on the MI data [12]. Next, we drew an illustration of the compositional diversity of the rock types based on these maps and the spectral band centers within the area of this study based on pyroxene data from the laboratory [13]. First, we classified the spectra roughly into pyroxene and plagioclase. Second, we classified the pyroxene layers by band center and depth of spectra, iron and titanium abundance, and topography. We estimated the thickness of each rock type layer. We observed the walls and floors of small craters that can be clearly recognized (i.e., exceeding 6 km in diameter) and confirmed which layer was exposed. We noted the distribution of these craters to estimate the area of each layer.

Results: Figure 1 represents part of the area that we investigated in this study. Here we present the RGB map (Fig. 1a) and FeO abundance map (Fig. 1b) that we used to determine the distribution of rock types (Fig. 1c). For instance, both two orange areas in Fig. 1a (white and black arrow) have low-Ca pyroxene composition spectrally but the area indicated black arrow is higher FeO abundance than the area indicated white arrow, and locates a central peak; therefore, we suggest that these two areas are different layers. In this way, we classified the rock types for six layers (orange, green, yellow, white, red, and blue). Orange represents the dominant LCP layer that is located around the central depression [10], green represents the HCP dominant layer located within the depression, and yellow represents an HCP dominant layer that has deeper absorption at 1050 nm and tends to have longer wavelengths in the band center. The yellow layer has higher iron content (about 14 wt%) than the green layer locat-

ed within the depression. The white layer has even longer wavelengths in the band center and higher iron content than the yellow layer (most of the band centers are greater than 1000 nm, and the iron content is more than 15 wt%) and is located within and around relatively large craters. The red layer is an LCP dominant layer in the central peaks of the large craters formed after the SPA basin impact. The navy blue layer is plagioclase.

We estimated the thicknesses of these layers based on the diameter and depth of the small craters and the original depth of the central peaks. From these results, orange layer thickness was estimated to be about 1.5 km in the central depression, the green layer was estimated to be about 6-7 km thick, and the yellow layer was estimated to be about 2 km. The red layer is at least 8 km thick, based on the diameters of the smallest and largest craters that have central peaks of the red layer. In terms of stratigraphy, we estimated from small craters that a green layer presents under orange, white and yellow layers, and the area of green layer is estimated at least 300,000 km². The red layer presents under the green layer.

Discussion: We estimated the origins of each layer. The orange layer (LCP layer) is interpreted to be mantle material ejected when the SPA basin formed. Because, from multiple observations, we found that this layer is consistent with the expanded mantle material found all over the SPA basin in a previous study [8]. The green layer (HCP layer) is the impact melt of the SPA basin. There are multiple reasons for this interpretation. If this layer is a monolith, it is larger and thicker than the mare basalt anywhere on the Moon in previous studies [14, 15, 16]. In addition, the average FeO abundance is 2 wt% lower than that of mare basalt [17]. From these reasons, it is possible that this layer is not

mare basalt, but rather is impact melt that pooled during formation of the SPA. The white layer is mare basalt. This layer location was approximately correlated with mare basalt observed in a previous study [18]. The yellow layer is a mixture of ancient mare basalt that erupted much earlier than the white mare basalt and the surrounding impact melt and/or mantle material ejecta. The green layer is much thinner than the 50 km impact melt of SPA inferred in previous studies [5], and the red layer (i.e. an LCP layer under the green layer) is different to the orange layer (upper mantle material) in FeO and TiO₂ abundances. Therefore, we interpret that the impact melt of the SPA is differentiated into the green layer and red layer.

Our study demonstrated the presence and distribution of impact melt generated by SPA impact event within the central part of the basin, and that the impact melt is differentiated into HCP and LCP layers.

References: [1] Garrick-Bethell and Zuber (2009) *Icarus*, 204, 399–408. [2] Spudis et al. (1994) *Science*, 266, 1848–1851. [3] Melosh. (1989), *Impact Cratering: A Geologic Process*, Oxford Univ.Press, London. [4] Lucey et al. (1998) *JGR*, 103, NO. E2, 3701–3708. [5] Vaughan et al. (2014) *PSS*, 91, 101–106 [6] Wilhelms et al. (1979) *USGS special*, report I-1162, [7] Ohtake et al. (2008) *EPS*, 60, 257–264. [8] Ohtake et al. (2014) *GRL*, 41, 2738–2745. [9] Pieters et al. (2001), *JGR*, 106, E11, 28,001–28,022. [10] Heiken et al. (1991), Cambridge University Press, 753p. [11] Lucey et al. (2000) *JGR*, 105, 20,297– 20,305. [12] Otake et al. (2012) *LPSC*,1905. [13] Klima et al. (2011) *MPS*, 46, Nr 3, 379–395. [14] Hiesinger et al. (2010) 115, E03003. [15] Williams and Zuber (1998) *Icarus*, 131, 107–122. [16] Thomson et al. (2009) 36, L12201. [17] Jolliff et al.(2000), *JGR*, vol.105, No.E2, 4197–4216. [18] Head and Wilson. (1992) *GCA*, 56, 2155–2175.

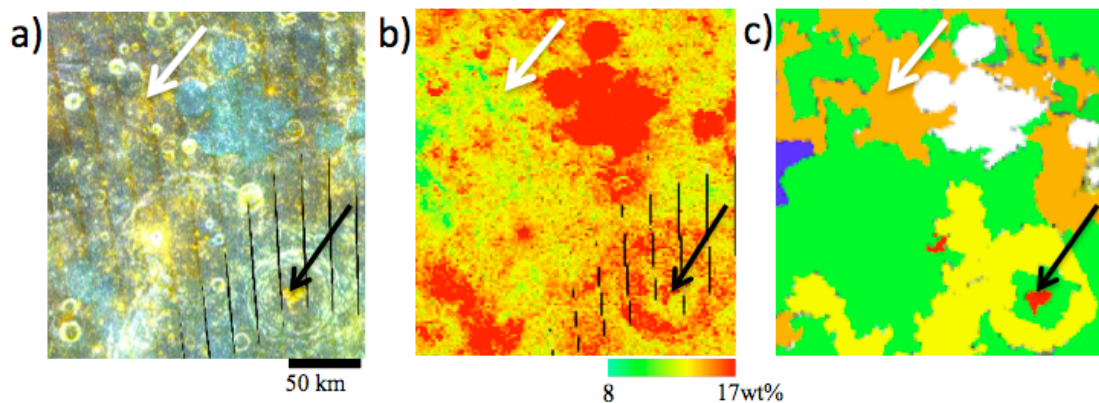


Fig. 1 Part of the area that we investigated in this study: RGB map (a), and FeO abundance map (b). We used these data to illustrate the distribution of rock types (c). (Regarding (c), orange is the mantle material, green is the upper impact melt, yellow is a mixture of impact melt and/or mantle material and mare basalt, red is the lower impact melt, and blue is crustal material.)